Oxygen Reduction

DOI: 10.1002/ange.201105204

Vertically Aligned BCN Nanotubes as Efficient Metal-Free Electrocatalysts for the Oxygen Reduction Reaction: A Synergetic Effect by Co-Doping with Boron and Nitrogen**

*Shuangyin Wang, Eswaramoorthi Iyyamperumal, Ajit Roy, Yuhua Xue, Dingshan Yu, and Liming Dai**

The oxygen reduction reaction (ORR) is an important process in many fields, including energy conversion (fuel cells, metal–air batteries),[1] corrosion,[2] and biosensing.[3] For fuel cells, the cathodic oxygen reduction is a major factor limiting their performance.[4] The ORR can proceed either through a four-electron process to directly combine oxygen with electrons and protons into water as the end product, or a less efficient two-step, two-electron pathway involving the formation of hydroperoxide ions as intermediate.[4] Oxygen reduction also occurs, albeit too slowly to be of any practical significance, in the absence of an ORR catalyst on the cathode. Platinum nanoparticles have long been regarded as the best catalyst for the ORR and are still commonly used in fuel cells due to their relatively low overpotential and high current density with respect to other commercial catalysts.[5] However, the ORR kinetics on the Pt-based electrode is sluggish,[5] and the Pt electrocatalyst still suffers from multiple drawbacks, such as susceptibility to fuel crossover from the anode, deactivation by CO, and poor stability under electrochemical conditions.[6] In addition, the high cost of Pt and its limited natural reserves are the major barriers to mass-market fuel cells for commercial applications.[5]

Recently, considerable efforts have been made to develop advanced electrocatalysts for reducing or replacing Pt-based electrodes in fuel cells.[7–10] In particular, certain nitrogen-doped carbon nanomaterials (e.g., carbon nanotubes (CNTs), graphene, porous carbon) were demonstrated to act as effective metal-free ORR electrocatalysts free from CO poisoning and crossover effect and having better long-term operational stability than commercially available Pt-based electrodes.[11–17] The enhanced catalytic activity of these metal-free nitrogen-doped carbon nanomaterials toward ORR could be attributed to the electron-accepting ability of nitrogen species, which creates net positive charges on adjacent carbon atoms to facilitate oxygen adsorption for ORR with low overpotential. The well-defined high surface area and intertube spacing for improved electrokinetics, as well as the good electrical and mechanical properties associated with vertically aligned N-doped carbon nanotubes (VA-NCNTs) provide additional benefits to the metal-free nanotube ORR electrode in achieving record electrocatalytic performance.[11] More recently, Yang et al.[17] reported boron-doped carbon nanotubes (BCNTs) as ORR electrocatalysts with improved activities relative to undoped CNTs. On the basis of experimental analyses and theoretical calculations, they concluded that the B atoms in the BCNT lattice are positively charged and act as the active sites for ORR.

In contrast to all-carbon nanotubes[18,19] carbon nanotubes containing both B and N atoms (BCN nanotubes),[20–23] either in an aligned or nonaligned form, are bandgap-tunable by means of their chemical composition.[22] Unlike CNTs, the bandgap of BCN nanotubes is independent of the diameter and chirality.[24–26] This unique structure–property relationship makes BCN nanotubes attractive candidates for potential uses in many areas where CNTs have been exploited.[20,27] In particular, the superb thermal stability and chemically tunable bandgap of BCN nanotubes provide tremendous opportunities to tune nanotube electronic properties for their use as an efficient metal-free ORR electrode, even at elevated temperatures.

Here we report, for the first time, metal-free ORR catalysts based on vertically aligned BCN (VA-BCN) nanotubes containing both B and N atoms and exploit possible synergetic effects of co-doping with B and N on the ORR activities by comparison with vertically aligned N-doped carbon nanotubes (VA-NCNTs) and vertically aligned B-doped carbon nanotubes (VA-BCNTs).

While synthesis of VA-CNTs have been widely reported,[18] there is much less discussion in the literature on the synthesis of VA-BCN nanotubes, most probably due to technical difficulties.[20–22] In most of the previous studies, ternary compounds (e.g., ferrocene, melamine, boron oxide) were used as precursors for nanotube synthesis by metal-catalyzed (e.g., Ni) thermal chemical vapor deposition (CVD), with and without plasma enhancement.[20–22] In the

[*] Dr. S. Wang,[+] Dr. E. Iyyamperumal,[+] Dr. Y. Xue, Dr. D. Yu, Prof. L. Dai
Department of Macromolecular Science and Engineering
Case Western Reserve University
10900 Euclid Avenue, Cleveland, Ohio 44106 (USA)
E-mail: Liming.Dai@case.edu
Dr. Y. Xue
On leave from: School of Ophthalmology & Optometry
Wenzhou Medical College, Zhejiang 325027 (China)
Dr. A. Roy
Thermal Science and Materials Branch, Materials & Manufacturing Directorate, Air Force Research Laboratory
Dayton, OH 45433 (USA)
[+] These authors contributed equally.

[**] This work was supported financially by AFOSR (FA 9550-10-1-0546) and MURI under Low Density Materials Program (Dr. Joycelyn Harrison–program Manager).

Supporting information for this article is available on the WWW under http://dx.doi.org/10.1002/anie.201105204.

current work, VA-BCN nanotubes were prepared by pyrolysis of melamine diborate, a single-compound source of carbon, boron, and nitrogen for BCN nanotube growth. Use of a single precursor compound simplifies the nanotube growth process. Melamine diborate was synthesized by treating melamine with boric acid (see Supporting Information). Detailed growth conditions for the VA-BCN nanotubes can be found in the Supporting Information, while the VA-NCNTs and VA-BCNTs were prepared according to reported procedures.[28,29]

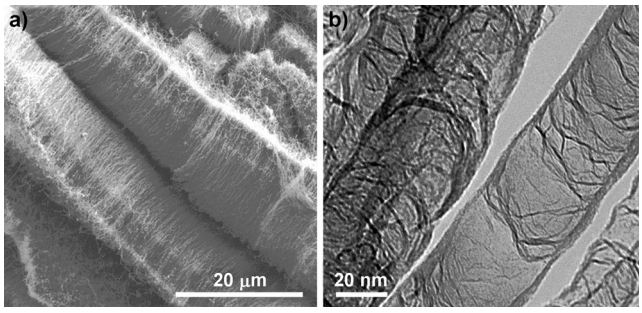

Figure 1. SEM (a) and TEM (b) images of VA-BCN nanotubes.

Figure 1a shows a typical SEM image (Hitachi S4800-F) of the VA-BCN nanotubes. The as-synthesized VA-BCN nanotubes are perpendicularly aligned on the SiO_2/Si substrate and almost free from pyrolytic impurities (e.g., carbon particles and other carbonaceous materials) with a fairly uniform length of about 15 μm. The length of the aligned nanotubes can be varied over a wide range (up to several tens of micrometers) in a controllable fashion by changing the experimental conditions (e.g., pyrolysis time, flow rate). The well-aligned relatively short VA-BCN nanotubes shown in Figure 1a could facilitate the diffusion of electrolyte ions and oxygen during the ORR process. Aligned morphologies of VA-BCNT and VA-NCNT were also observed (Figure S1, Supporting Information). High-resolution TEM (HRTEM, Zeiss, 300 kV) images of an individual BCN nanotube show a hollow tube of VA-BCN with an outer diameter of about 40 nm and a wall thickness of about 2–3 nm. The bamboo-like structure shown in Figure 1b is a characteristic feature of multiwalled BCN nanotubes.[20,22]

Electron energy loss spectroscopy (EELS) was used to characterize the K-edge absorption for B, C, and N. Typical EELS spectra from an individual BCN nanotube (Figure S2, Supporting Information) show three distinct absorption features at 188, 284, and 403 eV, which correspond to the expected B, C, and N K-edges, respectively,[22] and indicate successful incorporation of B, C, and N in the VA-BCN nanotubes. These results are further confirmed by X-ray photoelectron spectroscopic (XPS, VG Microtech ESCA 2000) measurements. As expected, the XPS survey spectra (Figure S3, Supporting Information) show B 1s, C 1s, and N 1s peaks for the VA-BCN nanotubes. Like many B-/N-doped nanotubes,[23] the presence of an O 1s peak in the VA-BCN nanotube sample is possibly due to the incorporation of physicochemically adsorbed oxygen,[30,31] which suggests an additional advantage as ORR electrode.[32] The absence of any metal peak in the XPS spectra shown in Figure S3 (Supporting Information) indicates that the metal catalyst particles formed at the bottom of each of the nanotubes during the "base-growth" process were completely removed upon mechanical removal of the nanotube sample from the growth substrate[33] and/or subsequent HCl washing (see Supporting Information). Among the chemically bonded C, B, and N atoms, the C content of VA-BCN (85.5%) dominates over B (4.2%) and N (10.3%), and the high C content in the VA-BCN nanotubes ensures high conductivity, compared to other BCN materials[34] for electrochemical applications, while the presence of B and N could significantly enhance the ORR activity (see below). Figures S4–S6 of the Supporting Information show high-resolution XPS, FTIR, and Raman spectra, from which more detailed chemical information can be obtained, as schematically shown in Figure S7 (Supporting Information).

All four electrode materials (i.e., VA-CNT, VA-NCNT, VA-BCNT, and VA-BCN nanotubes) showed a substantial reduction process in the presence of oxygen, whereas no obvious response was observed under nitrogen (Figure 2). The onset and peak potentials of ORR on the VA-BCNT, VA-NCNT, and VA-BCN nanotube electrodes are more positive, and the current densities much higher, than those on the VA-CNT electrode,[11] that is, heteroatom doping with N and/or B effectively improved the ORR activity. Comparison between VA-BCNT and VA-NCNT electrodes shows that N doping is more efficient than B doping for ORR in terms of the onset/peak potential and current density, though the VA-NCNT (4.1% N) prepared by pyrolysis of ferrocene under ammonia (see Supporting Information) used in this study did not show the record high ORR activity reported for its

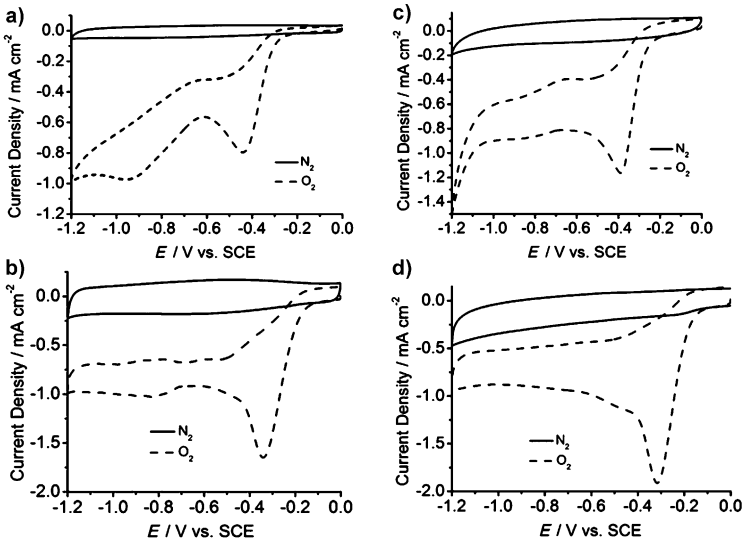

Figure 2. Cyclic voltammetry curves of a) VA-CNT, b) VA-BCNT, c) VA-NCNT, and d) VA-BCN electrodes in nitrogen- and oxygen-saturated 0.1 M KOH aqueous electrolyte solutions. The scan rate was 50 mV s^{-1}.

counterpart from pyrolysis of iron(II) phthalocyanine[11] due to its relatively low nitrogen content (see Supporting Information). Of the four electrodes investigated here, the VA-BCN nanotube electrode is most active in terms of the onset and peak potentials as well as the current density, that is, a synergetic effect resulted from co-doping of the carbon nanotubes with N and B. This is because not only both the isolated N and B atoms shown in Figure S7 (Supporting Information) can act as active sites for ORR through charge transfer with neighboring C atoms,[11,17] but also interaction between adjacent N and B atoms could facilitate charge transfer with neighboring C atoms, and hence further enhance the ORR performance of the VA-BCN nanotube electrode.

To gain further insight into the ORR on VA-BCN, VA-BCNT, VA-NCNT, and VA-CNT electrodes, rotating disk electrode (RDE) voltammetry (linear-sweep voltammetry, LSV) was performed in O_2-saturated 0.1 M KOH solution at a scan rate of 10 mV s^{-1} (Figure 3). For comparison, RDE tests

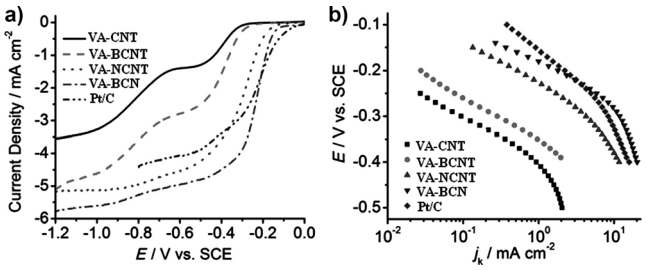

Figure 3. a) Linear-sweep voltammetry curves of various electrodes in oxygen-saturated 0.1 M KOH electrolyte at a scan rate of 10 mV s^{-1} and a rotation rate of 1000 rpm. b) Tafel plots derived from Figure 3 a in the low-current region.

were also performed on a commercial Pt/C electrode (C2-20, 20% platinum on Vulcan XC-72R; E-TEK). As shown in Figure 3 a, the typical two-step pathway was observed for the VA-CNT electrode at around −0.28 and −0.65 V, indicating a successive two-electron reaction pathway, instead of the direct four-electron pathway seen for the commercial Pt/C electrode. VA-BCNT shows a similar LSV profile to VA-CNT, but with a more positive onset potential and higher current density, and hence an overall better ORR activity. It is believed that boron doping could facilitate chemisorption of oxygen, which thus led to a relatively high catalytic activity toward ORR with respect to the VA-CNT electrode.[27,31] On the VA-NCNT and VA-BCN electrodes, the LSV curves show a single-step wide platform, indicating a four-electron ORR process. Interestingly, the half-wave potential (i.e., the potential at which the current is half of the limiting current) for ORR on the VA-CNT electrode in 0.1 M KOH solution of about −0.7 V (Figure 3 a) is much more negative than those of the other electrodes. The ORR current density from the VA-CNT electrode over the potential range covered is also much lower than those from other electrodes tested in this study. These results clearly indicate that B/N doping could significantly improve the electrocatalytic activity of the CNT electrodes toward ORR. On the other hand, the half-wave potential of the VA-BCN nanotube electrode (−0.25 V) is much more positive than that of VA-BCNT (−0.5 V) and VA-NCNT (−0.3 V), as shown in Figure 3 a. The diffusion current density from the VA-BCN electrode is also much higher than those from the VA-BCNT and VA-NCNT electrodes. Thus, the VA-BCN nanotube electrocatalysts showed the highest activity towards ORR among all nanotube electrodes studied in the present work. This again indicates a synergetic effect arising from co-doping of CNTs with both B and N atoms. Furthermore, Figure 3 a also shows an even more positive half-wave potential in LSV curves and higher diffusion current density for the VA-BCN nanotubes with respect to the Pt/C electrode.

Figure 3 b shows Tafel plots for ORR on various electrodes derived from Figure 3 a. The polarization curves in Figure 3 a were corrected for diffusion effects by using Equation (1)[35]

$$j_k = \frac{jj_D}{j_D - j} \tag{1}$$

where j_k is the kinetic current density, j_D the limiting current density, and j the measured current density. As seen in Figure 3 b, the Tafel plots clearly show the activity differences for the nanotube electrodes. At −0.3 V, for instance, the kinetic current density of ORR on the VA-BCN nanotubes is around 10.13 mA cm^{-2}, which is significantly higher than that of VA-CNT (0.10 mA cm^{-2}), VA-BCNT (0.28 mA cm^{-2}), and VA-NCNT (4.24 mA cm^{-2}) electrodes, and even slightly higher than that of Pt/C (8.34 mA cm^{-2}).

To further quantitatively characterize these nanotube electrodes, we used Equation (2) to calculate the transferred electron number n per oxygen molecule for each of the electrodes.[11,36]

$$n = \frac{4j_D}{j_D + \frac{j_R}{N}} \tag{2}$$

In this equation, j_D is the faradic disk current, j_R the faradic ring current (Figure 4 a–e), and N the collection efficiency (0.3) of the ring electrode.[11] Figure 4 f shows the dependence of n on the disk potential. The n value increases as the potential moves towards more negative values before reaching the limiting value of $n \approx 3.7$. As shown in Figure 4 f, ORR on the VA-CNT electrode proceeded via a 2e pathway in the low-overpotential region with generation of hydrogperoxide ions. Subsequent oxidation of hydrogen peroxide also followed a 2e pathway, leading to overall nearly 4e reaction in the high-overpotential region. Similar ORR kinetics was observed for the VA-BCNT electrode. On the VA-NCNT and VA-BCN electrodes, however, ORR followed a direct 4e pathway over the entire potential range by directly forming OH^- ions as final product, as is the case with the commercial Pt/C electrode. Thus, the VA-BCN nanotube electrode shows high diffusion current density, high positive half-wave potential, high electron transfer number (≈ 4), and high kinetic current density, which already outperforms the commercial Pt/C electrocatalysts for ORR in alkaline electrolyte.

In view of the potential of VA-BCNs as effective ORR catalysts to replace the commercially available Pt/C electrode,

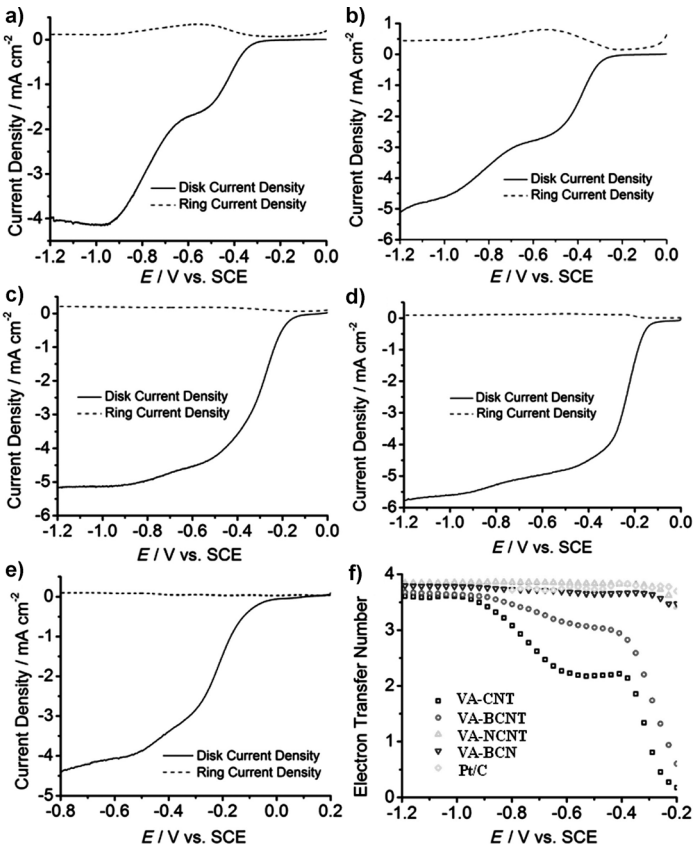

Figure 4. RRDE testing (LSV curves) of ORR on a) VA-CNT, b) VA-BCNT, c) VA-NCNT, d) VA-BCN, and e) Pt/C electrodes in oxygen-saturated 0.1 M KOH electrolyte at a scan rate of 10 mV s^{-1} and a rotation rate of 1000 rpm. f) Plot of electron-transfer number *n* against electrode potential.

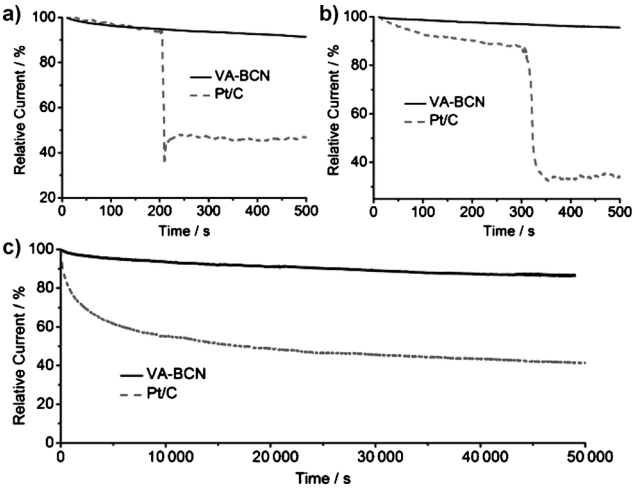

Figure 5. Chronoamperometric response for ORR at VA-BCN and Pt/C electrodes a) on addition of 3 M methanol after about 200 s and b) on introduction CO after about 300 s at −0.3 V. c) Durability evaluation of Pt/C and VA-BCN nanotube electrodes for 50000 s at −0.2 V and a rotation rate of 1000 rpm.

we further tested the electrochemical stability, possible methanol crossover, and CO poisoning. The current-time (*i*–*t*) chronoamperometric responses[12] for ORR at the VA-BCN and Pt/C electrodes (Figure 5) show a sharp decrease in current on addition of 3.0 M methanol for the Pt/C electrode (Figure 5a). In contrast, the amperometric response from the VA-BCN electrode remained almost uncharged even after the addition of methanol. Therefore, the VA-BCN electrode has a higher selectivity toward ORR and better methanol tolerance than the commercial Pt/C electrocatalyst. To examine CO poisoning, 10 vol% CO/O_2 was introduced into the electrolyte solution. As shown in Figure 5b, the VA-BCN electrode was insensitive to CO, whereas the Pt/C electrode was rapidly poisoned under the same conditions. Finally, the VA-BCN electrode was subjected to a chronoamperometric durability test for ORR in O_2-saturated 0.1 M KOH solution (Figure 5c). Continuous oxygen reduction (ca. 50000 s) at −0.2 V (vs. SCE) on the VA-BCN nanotube electrode caused only a slight loss (10%) of current density before leveling off. In contrast, the corresponding current loss on the Pt/C electrode under the same conditions was as high as about 60%. These results clearly indicate that the catalytically active sites on the VA-BCN nanotubes are much more stable than those on the commercial Pt/C electrode.

In summary, we have, for the first time, prepared vertically aligned BCN nanotubes by pyrolysis of melamine diborate, a single-compound source of carbon, boron, and nitrogen for BCN nanotube growth. Due to a synergetic effect arising from co-doping of CNTs with boron and nitrogen, the resultant VA-BCN nanotube electrode has higher electrocatalytic activity for ORR in alkaline medium than its counterparts doped with boron or nitrogen alone (i.e., VA-BCNT or VA-NCNT). The observed superior ORR performance with good tolerance to methanol and carbon monoxide and excellent durability for the VA-BCN nanotube electrode compared to a commercial Pt/C electrode opens up avenues for the development of novel, efficient, metal-free ORR catalysts by co-doping.

Received: July 25, 2011
Revised: August 23, 2011
Published online: October 11, 2011

Keywords: doping · electrochemistry · fuel cells · nanotubes · oxygen reduction

[1] B. C. H. Steele, A. Heinzel, *Nature* **2001**, *414*, 345.
[2] A. Goux, T. Pauport, D. Lincot, *Electrochim. Acta* **2006**, *51*, 3168.
[3] S. Gamburzev, P. Atanasov, E. Wilkins, *Sens. Actuators B* **1996**, *30*, 179.
[4] S. Basu, *Recent Trends in Fuel Cell Science and Technology*, Springer, Heidelberg, **2007**, p. 260.
[5] N. M. Marković, T. J. Schmidt, V. Stamenkovic, P. N. Ross, *Fuel Cells* **2001**, *1*, 105.
[6] M. Winter, R. J. Brodd, *Chem. Rev.* **2004**, *104*, 4245.
[7] Z. Peng, H. Yang, *J. Am. Chem. Soc.* **2009**, *131*, 7542.
[8] M.-H. Shao, K. Sasaki, R. R. Adzic, *J. Am. Chem. Soc.* **2006**, *128*, 3526.
[9] C. Wang, H. Daimon, T. Onodera, T. Koda, S. H. Sun, *Angew. Chem.* **2008**, *120*, 3644; *Angew. Chem. Int. Ed.* **2008**, *47*, 3588.

[10] V. R. Stamenkovic, B. Fowler, B. S. Mun, G. J. Wang, P. N. Ross, C. A. Lucas, N. M. Markovic, *Science* **2007**, *315*, 493.
[11] K. P. Gong, F. Du, Z. H. Xia, M. Durstock, L. M. Dai, *Science* **2009**, *323*, 760.
[12] R. L. Liu, D. Q. Wu, X. L. Feng, K. Mullen, *Angew. Chem.* **2010**, *122*, 2619; *Angew. Chem. Int. Ed.* **2010**, *49*, 2565.
[13] L. T. Qu, Y. Liu, J. B. Baek, L. M. Dai, *ACS Nano* **2010**, *4*, 1321.
[14] Y. Y. Shao, S. Zhang, M. H. Engelhard, G. S. Li, G. C. Shao, Y. Wang, J. Liu, I. A. Aksay, Y. H. Lin, *J. Mater. Chem.* **2010**, *20*, 7491.
[15] S. B. Yang, X. L. Feng, X. C. Wang, K. Müllen, *Angew. Chem.* **2011**, *123*, 5451; *Angew. Chem. Int. Ed.* **2011**, *50*, 5339.
[16] R. L. Liu, C. V. Malotki, L. Arnold, N. Koshino, H. Higashimura, M. Baumgarten, K. Mullen, *J. Am. Chem. Soc.* **2011**, *133*, 10372.
[17] L. Yang, S. Jiang, Y. Zhao, L. Zhu, S. Chen, X. Wang, Q. Wu, J. Ma, Y. Ma, Z. Hu, *Angew. Chem.* **2011**, *123*, 7270; *Angew. Chem. Int. Ed.* **2011**, *50*, 7132.
[18] H. Chen, A. Roy, J.-B. Baek, L. Zhu, J. Qu, L. Dai, *Mater. Sci. Eng. R* **2010**, *70*, 63.
[19] L. Dai, *Carbon Nanotechnology: Recent Developments in Chemistry, Physics, Materials Science and Device Applications*, Elsevier, Dordrecht, **2006**.
[20] X. D. Bai, E. G. Wang, J. Yu, H. Yang, *Appl. Phys. Lett.* **2000**, *77*, 67.
[21] D. Golberg, Y. Bando, M. Mitome, K. Kurashima, N. Grobert, M. Reyes-Reyes, H. Terrones, M. Terrones, *Chem. Phys. Lett.* **2002**, *360*, 1.
[22] W.-Q. Han, J. Cumings, A. Zettl, *Appl. Phys. Lett.* **2001**, *78*, 2769.
[23] K. Raidongia, D. Jagadeesan, M. Upadhyay-Kahaly, U. V. Waghmare, S. K. Pati, M. Eswaramoorthy, C. N. R. Rao, *J. Mater. Chem.* **2008**, *18*, 83.
[24] N. Hamada, S.-I. Sawada, A. Oshiyama, *Phys. Rev. Lett.* **1992**, *68*, 1579.
[25] R. Saito, M. Fujita, G. Dresselhaus, M. S. Dresselhaus, *Phys. Rev. B* **1992**, *46*, 1804.
[26] X. Blase, A. Rubio, S. G. Louie, M. L. Cohen, *Phys. Rev. B* **1995**, *51*, 6868.
[27] X. Wei, M.-S. Wang, Y. Bando, D. Golberg, *J. Am. Chem. Soc.* **2010**, *132*, 13592.
[28] Y. T. Lee, N. S. Kim, S. Y. Bae, J. Park, S.-C. Yu, H. Ryu, H. J. Lee, *J. Phys. Chem. B* **2003**, *107*, 12958.
[29] C. F. Chen, C. L. Tsai, C. L. Lin, *Diamond Relat. Mater.* **2003**, *12*, 1500.
[30] P. G. Collins, K. Bradley, M. Ishigami, A. Zettl, *Science* **2000**, *287*, 1801.
[31] D. W. Wang, F. Li, Z.-G. Chen, G. Q. Lu, H.-M. Cheng, *Chem. Mater.* **2008**, *20*, 7195.
[32] S. Wang, D. Yu, L. Dai, *J. Am. Chem. Soc.* **2011**, *133*, 5182.
[33] K. Hata, D. N. Futaba, K. Mizuno, T. Namai, M. Yumura, S. Iijima, *Science* **2004**, *306*, 1362.
[34] J. Yu, J. Ahn, S. F. Yoon, Q. Zhang, R. B. Gan, K. Chew, M. B. Yu, X. D. Bai, E. G. Wang, *Appl. Phys. Lett.* **2000**, *77*, 1949, and references therein.
[35] Q. Zhou, C. M. Li, J. Li, J. Lu, *J. Phys. Chem. C* **2008**, *112*, 18578.
[36] D. Yu, Q. Zhang, L. Dai, *J. Am. Chem. Soc.* **2010**, *132*, 15127.

